Biogeosciences, 5, 1007–1022, 2008
www.biogeosciences.net/5/1007/2008/

Biogeosciences

Coupling of heterotrophic bacteria to phytoplankton bloom development at different pCO_2 levels: a mesocosm study

M. Allgaier[1,*], U. Riebesell[2], M. Vogt[3], R. Thyrhaug[4], and H.-P. Grossart[1]

[1]Leibniz-Institute of Freshwater Ecology and Inland Fisheries; Department Limnology of Stratified Lakes; Alte Fischerhuette 2; D-16775 Stechlin-Neuglobsow, Germany
[2]Leibniz- Institute for Marine Sciences, University of Kiel, Duesternbrooker Weg 20, D-24105 Kiel, Germany
[3]Laboratory for Global Marine and Atmospheric Chemistry, School of Environmental Sciences, University of East Anglia, Norwich NR 7TJ, UK
[4]Department of Biology, Jahnebakken 5, University of Bergen, Norway
[*]currant address: DOE Joint genome Inst., Microbial Ecology Program, 2800 Mitchell Drive, Walnut Creek, CA 94598, USA

Received: 13 November 2007 – Published in Biogeosciences Discuss.: 29 January 2008
Revised: 18 June 2008 – Accepted: 19 June 2008 – Published: 21 July 2008

Abstract. The predicted rise in anthropogenic CO_2 emissions will increase CO_2 concentrations and decrease seawater pH in the upper ocean. Recent studies have revealed effects of pCO_2 induced changes in seawater chemistry on a variety of marine life forms, in particular calcifying organisms. To test whether the predicted increase in pCO_2 will directly or indirectly (via changes in phytoplankton dynamics) affect abundance, activities, and community composition of heterotrophic bacteria during phytoplankton bloom development, we have aerated mesocosms with CO_2 to obtain triplicates with three different partial pressures of CO_2 (pCO_2): 350 μatm ($1\times CO_2$), 700 μatm ($2\times CO_2$) and 1050 μatm ($3\times CO_2$). The development of a phytoplankton bloom was initiated by the addition of nitrate and phosphate. In accordance to an elevated carbon to nitrogen drawdown at increasing pCO_2, bacterial production (BPP) of free-living and attached bacteria as well as cell-specific BPP (csBPP) of attached bacteria were related to the C:N ratio of suspended matter. These relationships significantly differed among treatments. However, bacterial abundance and activities were not statistically different among treatments. Solely community structure of free-living bacteria changed with pCO_2 whereas that of attached bacteria seemed to be independent of pCO_2 but tightly coupled to phytoplankton bloom development. Our findings imply that changes in pCO_2, although reflected by changes in community structure of free-living bacteria, do not directly affect bacterial activity. Furthermore, bacterial activity and dynamics of heterotrophic bacteria, especially of attached bacteria, were tightly correlated to phytoplankton development and, hence, may also potentially depend on changes in pCO_2.

Correspondence to: H.-P. Grossart
(hgrossart@igb-berlin.de)

1 Introduction

Many recent studies on phytoplankton carbon acquisition mechanisms indicate large effects on physiology and composition of phytoplankton due to on-going changes in aquatic pCO_2 (e.g. Burkhart et al., 2001; Tortell et al., 2002). The expected change in pCO_2 will result in a pH drop by ca. 0.35 units by the year 2100 (Wolf-Gladrow et al., 1999) and may even drop by 0.7 units over the next two centuries (Caldeira and Wickett, 2003). This may result in a significant reduction of biogenic calcification, in particular of coccolithophores (Riebesell et al., 2000), a higher loss of POC (Engel et al., 2005), and changes in particle flux to deeper waters (Armstrong et al., 2002; Klaas and Archer, 2002). Due to changes in phytoplanktonic production of extracellular organic matter concentration of TEP may increase with increasing pCO_2 (Engel et al., 2004). Thus, changes in pCO_2 may also affect the C:N ratio of the algae and, hence, degradability of phytoplankton derived DOC and POC in the ocean. Although it has been shown for terrestrial ecosystems that increasing levels of pCO_2 often lead to increased bacterial numbers and activities (Zak et al., 2000), which are related to increasing photosynthetic exudation or changes in peroxidase activities,

there is hardly any comparable study available for marine ecosystems. In a previous mesocosm study (Grossart et al., 2006b) we indeed found a measurable but indirect effect of changes in pCO_2 on bacterial abundance and activities. This effect was mainly linked to algal and presumably particle dynamics.

Senescent planktonic algae and aggregates are rapidly colonized by bacteria (e.g. Smith et al., 1995; Simon et al., 2002) which have a repertoire of hydrolytic enzymes (Hoppe et al., 1993; Martinez et al., 1996) for efficient POM solubilisation to DOM (Smith et al., 1992; Grossart and Ploug, 2001). Even though DOM of algal origin can be rapidly used by bacteria (Grossart et al., 2006a), a seasonal accumulation of DOM in the oceanic photic zone is commonly observed (Williams, 1995) and may indicate a semi-labile nature of the released dissolved organic carbon (DOC; Søndergaard et al., 2000). A substantial fraction (25 to 35%) of DOC released from phytoplankton can even resist microbial degradation for years (Fry et al., 1996). Alternatively to low bioavailability, temporary accumulation of POC and DOC has been explained by a "malfunctioning microbial loop", e.g. when nutrient availability limits bacterial growth and viral lysis as well as grazing the bacterial biomass (Thingstad et al., 1997; Williams, 1995). However, it has been suggested that viruses primarily influence bacterial community composition, while grazers have a greater impact on total bacterial biomass (Thingstad, 2000).

On the other hand, DOM released by phytoplankton affect formation of particles, such as transparent exopolymer particles (TEP) and aggregates (Grossart et al., 2006a). Most notably, TEP have been identified as an important agent for aggregation (Passow, 2002). Various studies have shown that TEP are produced by planktonic algae, but also by bacteria and from dissolved precursor material (Zhou et al., 1998; Passow, 2002; Engel et al., 2004). Those processes, however, greatly depend on the physiological state of the algae (Grossart et al., 2006a).

Hence, the main purpose of the present study was to evaluate whether the expected future changes in pCO_2 will change abundance, activities, and community structure of heterotrophic bacteria during the build up and decline of a phytoplankton bloom. We wanted to test whether heterotrophic bacteria are directly affected by changes in pCO_2 or more indirectly react to pCO_2 induced changes in phytoplankton bloom development (as has been proposed by our earlier paper; Grossart et al., 2006b). This paper is part of a larger mesocosm study on the effects of CO_2 induced seawater acidicication on complex plankton communities. An overview of all studies performed and their major results are given by Riebesell et al. (2008).

2 Materials and methods

2.1 Experimental set up and sampling

The mesocosm study was performed between 15 May and 9 June 2005 at the Espegrend Marine Biological Station (at Raunefjorden, 60.2° N, 5.1° E) of the University of Bergen, Norway. Nine polyethylene enclosures ($\sim$27 m^3, 9.5 m water depth) were moored to a raft equipped with a small floating laboratory. The enclosures were simultaneously filled with unfiltered, nutrient-poor, post-bloom fjord water from 13.5 m depth. To avoid disturbances by faecal matter of seabirds and to maintain headspaces at target pCO_2, the enclosures were covered by gas-tight tents made of ETFE foil, which allowed for 95% light transmission of the complete spectrum of sunlight. The mesocosms were aerated with CO_2 to obtain triplicates of three different levels, 350 μatm ($1\times CO_2$), 700 μatm ($2\times CO_2$) and 1050 μatm ($3\times CO_2$) (for details see Riebesell et al., 2007; Schulz et al., 2008). Continuous flushing of the tents with air adjusted to target CO_2 concentrations ensured that starting values were kept in the headspace throughout the experiment. The addition and subsequent mixing of 800 litres of freshwater into the upper 5.5 m of the mesocosms, resulted in water column stratification with a salinity gradient of 1.5 between the surface mixed layer (S=30.5) and the underlying water column. A homogenous distribution of dissolved compounds was achieved by continuous mixing of the upper layer by peristaltic pumps (flow rate 450 l h^{-1}). The development of a phytoplankton bloom was initiated by the addition of nitrate and phosphate (initial concentrations of 14 μmol l^{-1} NO_3 and 0.7 μmol l^{-1} PO_4). The experiment started at a post-bloom $Si(OH)_4$ level of 3.2 μmol l^{-1}. Development and decline of the phytoplankton bloom was monitored daily over a 24 day period. Depth-integrated water samples were taken daily at 10 a.m. by means of a 5 m long, 8 cm diameter tube which was lowered into the mesocosms, closed at the top, pulled up onto the raft and emptied into sampling bottles. Bottles were stored until further processing in a cold room adjusted to the in situ temperature of the fjord. For comparison water samples were also taken from the adjacent fjord at the same depth.

Throughout the whole experiment a multitude of environmental parameters, such as NO_3, PO_4, $Si(OH)_4$, particulate organic carbon (POC), C:N ratio, transparent exopolymer particles (TEP), algal abundance, chlorophyll-*a* (Chl-*a*), dissolved organic carbon (DOC) (see Schulz et al., 2008), primary production (PrProd), and viral abundance (Larsen et al., 2008) were continuously monitored. Particulate and dissolved dimethylsulfoniopropionate ($DMSP_p$ and $DMSP_d$, respectively), and dimethyl-sulphide (DMS) were measured by Vogt et al. (2008).

2.2 Bacterial numbers

For enumeration of free and particle-associated bacteria 1 or 5 ml of seawater were filtered onto black 0.2 and 5.0 μm pore size Nuclepore membranes, respectively. The filters were stained with SYBR Gold (Invitrogen) and stored frozen at –20°C until counting. Bacteria were counted by epifluorescence microscopy (DR-MB, Leica, Germany) at 1000× magnification. The number of free bacteria was calculated by subtracting the number of particle-associated bacteria (5.0 μm filters) from that of total bacteria (0.2 μm filters). Comparison with flow cytometry (Paulino et al., 2008) indicated that our numbers were overestimated due to the presence of big viruses within a size range of 100 to 200 nm which could not be reliably distinguished from bacteria by epifluorescence microscopy. Therefore, the abundance of free-living bacteria has been corrected for the abundance of big viruses.

2.3 Bacterial production

Rates of bacterial protein production (BPP) were determined by incorporation of ^{14}[C]-leucine (^{14}C-Leu, Simon and Azam, 1989). Triplicates and a formalin-killed control were incubated with ^{14}C-Leu (1.15×10^{10} Bq mmol^{-1}, Amersham, England) at a final concentration of 50 nmol l^{-1}, which ensured saturation of uptake systems of both free and particle-associated bacteria. Incubation was performed in the dark at in situ temperature (9 to 11.5°C) for 1 h. After fixation with 2% formalin, samples were filtered onto 5.0 μm (attached) and 0.2 μm (total isotope incorporation) nitrocellulose filters (Sartorius, Germany) and extracted with ice-cold 5% trichloroacetic acid (TCA) for 5 min. Thereafter, filters were rinsed twice with ice-cold 5% TCA, once with ethanol (96% v/v), and dissolved with ethylacetate for measurement by liquid scintillation counting. Standard deviation of triplicate measurements was usually <15%. BPP of free bacteria was calculated by subtraction of attached BPP from total BPP. The amount of incorporated ^{14}C-Leu was converted into BPP by using an intracellular isotope dilution factor of 2. A conversion factor of 0.86 was used to convert the protein produced into carbon (Simon and Azam, 1989). Cell-specific BPP was calculated for both bacterial fractions by taking the respective cell numbers into account.

2.4 DNA extraction and PCR amplification of 16S rRNA gene fragments

Particle-associated and free-living bacteria were separated by sequential filtration of the water samples throughout 5.0 and 0.2 μm Nuclepore polycarbonate filters, respectively. Particle-associated bacteria were retained by filtering 150 ml of sample onto a 5.0 μm Nuclepore membrane, whereas free-living bacteria were collected by filtering 100 ml of the 5.0 μm filtrate onto a 0.2 μm Nuclepore membrane. Filters were transferred into sterile Eppendorf tubes and kept frozen at –20°C until pending DNA extraction. Extraction of genomic DNA was performed, using a standard protocol with phenol/chloroform/isoamylalcohol, SDS, polyvinylpyrrolidone, and zirconium beads as described previously (Allgaier and Grossart, 2006a).

For denaturing gradient gel electrophoresis (DGGE) a 550 bp fragment of the 16S rRNA gene was amplified using the primer pair 341f and 907r (5′ – CCT ACG GGA GGC AGC AG – 3′ and 5′ – CCG TCA ATT CMT TTG AGT TT – 3′, Muyzer et al., 1998). At the 5′-end of the primer 341f an additional 40 bp GC-rich nucleotide sequence (GC-clamp) was added to stabilize migration of the DNA fragment in the DGGE (Muyzer et al., 1993). The PCR reaction mixture contained: 2 to 5 μl template DNA, each primer at a concentration of 200 nM, each deoxyribonucleoside triphosphate at a concentration of 250 μM, 2 mM $MgCl_2$, 5 μl of 10× PCR reaction buffer, and 0.5 U of BIOTAQ Red DNA Polymerase (Bioline) in a total volume of 50 μl. PCR amplification was performed with a Gradient Cycler PT-200 (MJ Research) using the following conditions: initial denaturation at 95°C (3 min), followed by 30 cycles of denaturation at 95°C (1 min), annealing at 55°C (1 min), and extension at 72°C (2 min). A final extension at 72°C for 10 min completed the reaction.

2.5 Denaturing gradient gel electrophoresis (DGGE) and sequencing

DGGE was performed as described previously (Allgaier and Grossart, 2006b) in a 7% (v/v) polyacrylamide gel with a denaturing gradient from 40 to 70% of urea and formamide. Prior loading of PCR products onto DGGE gels, DNA was quantified on agarose gels using a quantitative DNA ladder (Low DNA Mass Ladder, Invitrogen) and similar amounts of DNA were loaded onto the DGGE gels. DGGE gels were run in 1× TAE electrophoresis buffer (40 mM Tris-HCl (pH 8.3), 20 mM acetic acid, 1 mM EDTA) for 20 h at a constant voltage of 100 V and a constant temperature of 60°C. The gels were stained with 1 x SYBR Gold (Invitrogen) and documented using an AlphaImager 2200 Transilluminator (Biozym).

For sequencing, several DGGE bands were excised and incubated over night at 35°C in elution buffer (0.5 M Ammonia acetate, 1 mM EDTA). Eluted DNA fragments were precipitated using 0.3 vol. 7.5 M ammonia acetate and 0.7 vol. isopropanol and purified with 70% ethanol. DNA fragments were sequenced as described previously (Allgaier and Grossart, 2006a) using primers 341f and 907r.

2.6 Analyses of DGGE profiles

DGGE banding patterns were analyzed by using the Software packages GelCompar II version 3.5 (Applied Maths) and PRIMER 5, version 5.2.9 (PRIMER-E Ltd.). Within

GelCompar II first a band based binary presence/absence table was calculated applying Dice similarity coefficient. This presence/absence table was imported into the software PRIMER 5 and used for hierarchical clustering analyses and analyses of similarity (ANOSIM). To avoid distortions originating from non-normal distribution of the species data of the DGGE gels we used a Bray-Curtis similarity matrix for cluster analyses and ANOSIM rather than the original data matrix. For cluster analyses the *complete linkeage* algorithm was used provided by the software package. This algorithm calculates distances between clusters (Clarke and Gorley, 2001).

2.7 Phylogenetic analysis

Phylogenetic analyses of the partial 16S rRNA gene sequences were done using the ARB software package (http://www.arb-home.de). The retrieved sequences were imported into an ARB database of 52 000 reference sequences including the closest related sequences determined by BLAST (http://www.ncbi.nlm.nih.gov/BLAST/). Sequences were first aligned automatically by the integrated alignment module within the ARB package and subsequently corrected manually. For stability of the phylogenetic tree a backbone tree was calculated comprising only sequences of $\geq$1400 nucleotides. Sequences $\leq$1400 nucleotides were added afterwards to the tree according to maximum parsimony criteria. Consistence of branching patterns was checked applying the three phylogenetic reconstruction methods: neighbor-joining, maximum parsimony, and maximum likelihood to the appropriate set of sequences. The final tree was calculated using the maximum likelihood algorithm.

2.8 Nucleotide sequence accession numbers

Partial sequences of 16S rRNA gene fragments obtained in this study have been deposited in GenBank with the following accession numbers: EU179278 – EU179311.

2.9 Statistical analysis

In order to determine if measured parameters over time differed significantly between pCO_2 levels,statistical analyses were done by repeated measures ANOVA for analyzing the treatment effect using the software SPSS 9.0. If the sphericity of the variance-covariance matrix was violated the degrees of freedom were altered according to the Mauchly test using Greenhouse Geisser Epsilon. Furthermore, we used the "linear regression" module of the SPSS 9.0 software. All regressions were tested for dependency on pCO_2 by applying the CHOW test with univariate GLM. This determines if the regression parameters are different between different pCO_2 levels. Dependencies of bacterial parameters from other environmental parameters were tested by "stepwise" multiple regression analysis. Significance was given at values <0.05.

To test the significance of differences between the DGGE banding patterns ANOSIM (Clarke and Green, 1988) was applied. ANOSIM generates a test statistic (R) which is an indication of the degree of separation between groups. A score of 1 indicates complete separation whereas a score of 0 indicates no separation. DGGE banding patterns were also analyzed by non-metric multidimensional scaling (NMS) ordinations using the software package PC-ORD, Version 4.0 (MJM Software Design). Similar to ANOSIM a binary presence/absence table was used for all NMS analyses. The advantage of NMS over other multivariate statistical methods (e.g. canonical correspondence analysis, CCA) is that this method uses rank order information of a similarity matrix of the samples rather than the original data matrix. Thus, NMS avoids distortions originating from the non-normal distribution of the species data of the DGGE gels (McCune and Grace, 2002).

3 Results

3.1 Bacterial abundance

Abundances of either free-living or attached bacteria were almost identically among all mesocosms irrespective of their pCO_2 (Fig. 1a and b). Except for high abundances at the beginning of the experiment, free-living bacteria reached a pronounced maximum of ca. 5 to 6×10^6 cells ml^{-1} between days 12 and 16 (Fig. 1a) during the decline of the algal bloom. Abundances of free-living bacteria dropped to a low of ca. 1 to 3×10^6 cells ml^{-1} between days 18 and 20 and thereafter increased to ca. 3 to 6×10^6 cells ml^{-1} at the end of the experiment when dinoflagellate and cyanobacterial abundances increased. Numbers of attached bacteria were lower and showed a different temporal pattern (Fig. 1b). Numbers of attached bacteria were relatively high at the beginning of the experiment but declined until day 6. Attached bacteria reached a maximum of 0.28 to 0.42×10^6 cells ml^{-1} between days 10 to 14, slightly earlier than free-living bacteria. Thereafter, they slowly decreased to $\sim$0.20 to 0.23×10^6 cells ml^{-1} at the end of the experiment.

3.2 Bacterial protein production (BPP)

BPP of both free-living and attached bacteria followed primary production (Egge et al., 2007) with a lapse of ca. 2 days (Fig. 2a and b). BPP of free-living bacteria increased from day 6 on and varied between 1.5 and 3.2 μg C l^{-1} h^{-1} on day 10 and further increased until day 14 to 2.8 to 3.9 μg C l^{-1} h^{-1} (Fig. 2a). BPP of free-living bacteria was low (ca. 0.4 to 1.4 μg C l^{-1} h^{-1}) between days 18 and 22 and only slightly increased at the end of the experiment. BPP of attached bacteria increased slightly earlier (between days 6 and 8) but much steeper (3.1 to 4.8 μg C l^{-1} h^{-1}) than that of free-living bacteria (Fig. 2b). A second peak occurred on day 14 in parallel to that of free-living bacteria and reached 2.9

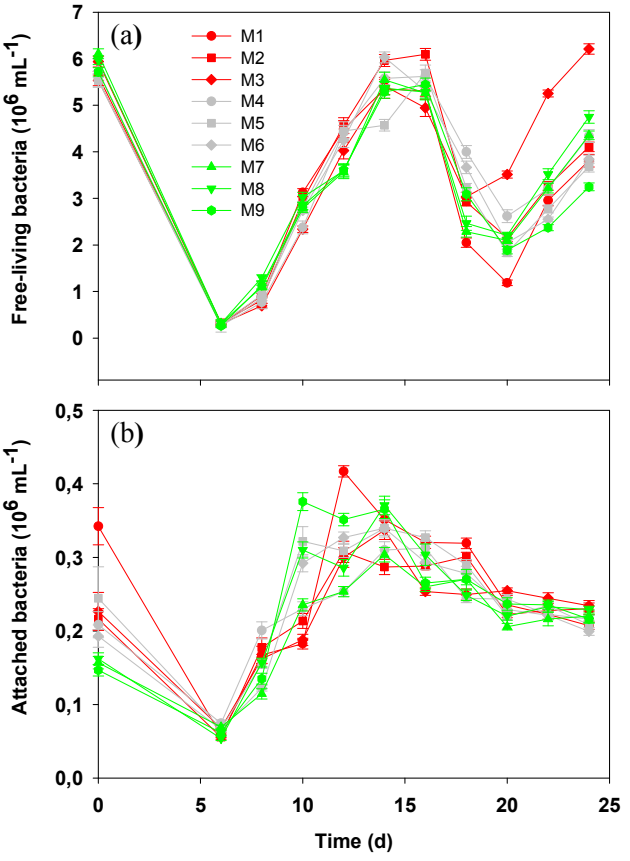

Fig. 1. **(a)** Abundance of free-living ($\leq$5.0 μm$\geq$0.2 μm) and **(b)** attached bacteria ($\geq$5.0 μm). M1–M3 mesocosms with 3×CO_2, M4–M6 mesocosms with 2×CO_2, and M7–M9 mesocosms with 1×CO_2.

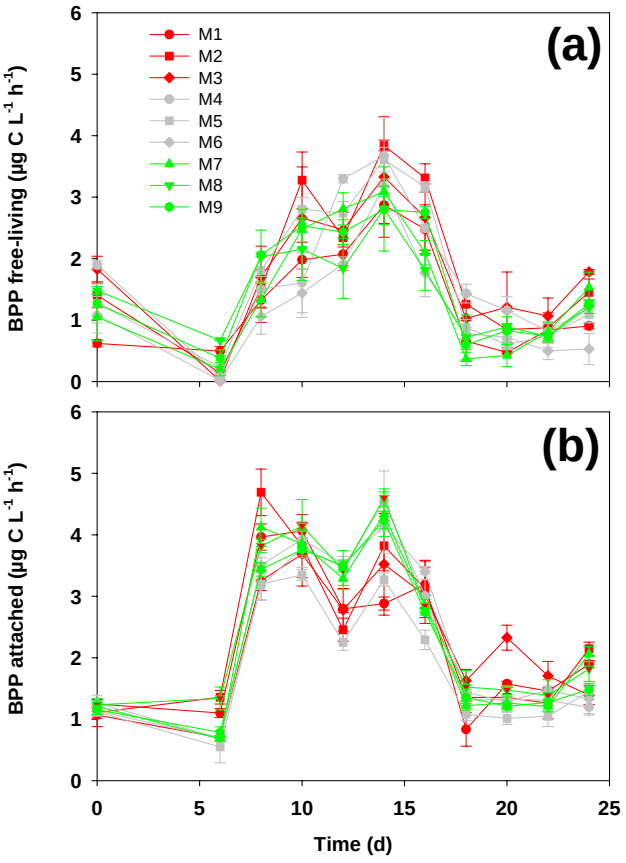

Fig. 2. Bacterial protein production (BPP) of **(a)** free-living ($\leq$5.0 μm$\geq$0.2 μm) and **(b)** attached bacteria ($\geq$5.0 μm). M1–M3 mesocosms with 3×CO_2, M4–M6 mesocosms with 2×CO_2, and M7–M9 mesocosms with 1×CO_2.

to 4.6 μg C l^{-1} h^{-1}. Similarly to free-living bacteria, BPP of attached bacteria was rather low (0.9 to 2.2 μg C l^{-1} h^{-1}) between days 18 and 22 and slightly increased at the end of the experiment.

3.3 Cell-specific bacterial protein production (csBPP)

csBPP of both free-living and attached bacteria showed a similar temporal pattern but greatly differed in magnitude (Fig. 3a and b). A pronounced maximum of csBPP of free-living bacteria occurred on days 6 to 8 (1.1 to 2.4 fg C cell^{-1} h^{-1}, Fig. 3a) almost in parallel to the first peak in primary production indicating a strong coupling between phytoplankton growth and bacterial activity. However, csBPP of free-living bacteria was rather low (0.6 to 0.8 fg C cell^{-1} h^{-1}) during and shortly after the second peak in primary production. Thereafter, csBPP of free-living bacteria continuously decreased towards the end of the experiment. CsBPP of attached bacteria increased in parallel to primary production and reached a first peak (16 to 36 fg C cell^{-1} h^{-1}) on days 6 to 8. In parallel to csBPP of free-living bacteria, csBPP of attached bacteria was also lower (7 to 14 fg C cell^{-1} h^{-1}) during and shortly after the second peak in primary production. CsBPP of attached bacteria further dropped (to 3 to 10 fg C cell^{-1} h^{-1}) between days 18 and 24 when primary production and phytoplankton abundance was rather low.

3.4 Statistical analysis

None of the parameters tested by repeated measures ANOVA revealed a statistically significant dependency on pCO_2 (data not shown). Linear regression analysis between measured bacterial parameters and environmental variables, however, revealed several highly significant relationships (Table 1). Abundance as well as BPP of both free-living and particle-associated bacteria were negatively correlated to NO_3, PO_4, and $Si(OH)_4$ indicating that bacterial abundance and BPP were closely correlated to the temporal course of phytoplankton development. The positive relationships between NO_3

Table 1. Linear regression analysis between measured bacterial parameters and environmental variables. BPP free/attached (bacterial production of free and attached bacteria, respectively), cs BPP free/attached (cell-specific BPP of free and attached bacteria, respectively), Bacteria free/attached (abundance of free-living and attached bacteria, respectively), NO_3, PO_4, $Si(OH)_4$, POC (particulate organic carbon), C:N (C:N ratio of particulate matter), TEP (transparent exopolymer particles), Chl-*a* (chlorophyll-*a*), Ehux (coccolithophore *Emiliania huxleyi*), Diatoms (diatoms primarily *Skeletonema costatum* and *Nitzschia longissima*), Cyano (cyanobacteria), PrProd (primary production), Virus (total virus), Big Virus (distinct group of big virus with a size of up to 200 nm), DOC (dissolved organic matter), DMSP (dimethylsulfoniopropionate), DMS (dimethylsulfide), ns (not significant), for TEP n=89, for POC and C:N n=87, for NO_3, PO_4, Si n=80, for DOC n=72, for $DMSP_d$ n=88, for all other parameter n=90.

Parameter	BPP free T-, p-value	BPP attached T-, p-value	csBPP free T-, p-value	csBPP attached T-, p-value	Bacteria free T-, p-value	Bacteria attached T-, p-value
NO_3	–2.309, 0.024	ns	3.348, 0.001	8.915, <0.001	–12.778, <0.001	–8.647, <0.001
PO_4	–6.239, <0.001	–4.958, <0.001	–2.785, 0.007	ns	–8.243, <0.001	–10,898, <0.001
$Si(OH)_4$	–4.165, <0.001	ns	ns	6.124, <0.001	–14.181, <0.001	–13,761, <0.001
POC	10.869, <0.001	5.342, <0.001	ns	ns	12.117, <0.001	12.074, <0.001
C:N	2.768, 0.007	2.104, 0.038	ns	ns	3.149, 0.002	5.447, <0.001
TEP	5.97, <0.001	2.098, 0.039	ns	–4.885, <0.001	10.256, <0.001	13.365, <0.001
Chl-*a*	8.513, <0.001	9.395, <0.001	6.446, <0.001	3.495, 0.001	ns	3.665, <0.001
Ehux	4.881, <0.001	7.280, <0.001	7.459, <0.001	5.659, <0.001	ns	ns
Diatoms	3.922, <0.001	6.656, <0.001	6.756, <0.001	5,481, <0.001	ns	ns
Cyano	–3.403, 0.001	–5.902, <0.001	–6.066, <0.001	–6.555, <0.001	2.546, 0.013	ns
PrProd	4.212, <0.001	9.256, <0.001	13.146, <0.001	9.168, <0.001	ns	ns
Virus	–3.622, <0.001	–6.525, <0.001	–7.139, <0.001	–7.873, <0.001	2.38, 0.022	ns
Big Virus	–9.041, <0.001	–12.581, <0.001	–9.139, <0.001	–3.993, <0.001	–2.730, 0.008	–4.553, <0.001
DOC	–2.208, 0.046	–3.906, <0.001	–4.083, <0.001	–6.360, <0.001	2.052, 0.044	2.319, 0.036
$DMSP_d$	6.856, <0.001	3.993, <0.001	ns	ns	7.558, <0.001	5.915, <0.001
$DMSP_p$	16.984, <0.001	9.591, <0.001	4.742, <0.001	ns	7.208, <0.001	8.157, <0.001
DMS	11.361, <0.001	8.547, <0.001	5.131, <0.001	ns	4.885, <0.001	6.616, <0.001

and csBPP of both free-living and attached bacteria, however, may indicate a direct dependency of bacterial activity on NO_3 availability.

BPP and csBPP of both free-living and attached bacteria were positively correlated to almost all algal parameters (chlorophyll-*a* (Chl-*a*), abundances of *Emiliania huxleyi* (Ehux) and diatoms (Diatoms), primary production (PrProd), dissolved and particulate dimethylsulfoniopropionate ($DMSP_p$ and $DMSP_d$, respectively), and dimethylsulfide (DMS) but negatively correlated to abundances of cyanobacteria (Cyano), total viruses (Virus), virus in the size range of 100 to 200 nm (Big Virus), and surprisingly to DOC. POC and C:N ratio of the suspended matter were positively correlated to BPP but not to csBPP of free-living and attached bacteria suggesting that increased POC and C:N ratios do not affect the activity of individual cells but set an activity level for total bacteria. CsBPP of attached bacteria was negatively correlated to TEP. Bacterial numbers (both free-living and attached), however, were positively related to POC, C:N, TEP, DOC, and $DMSP_{p+d}$ (and DMS) indicating that the presence of potential bacterial substrates lead to increases in bacterial abundance.

To reduce the number of significant correlations between measured bacterial and environmental variables we have used a stepwise multiple regression analysis (Table 2). For particulates (Table 2a) the analysis revealed that BPP of free-living and attached bacteria was tightly correlated to $DMSP_p$. Additionally, BPP of attached bacteria was negatively correlated with TEP and positively with C:N ratio of particulates. CsBPP of free-living was exclusively positively correlated to Ehux whereas csBPP of attached bacteria was negatively related to the abundance of Cyano and TEP and positively to $DMSP_p$. Abundance of free-living bacteria was positively related to POC, Cyano, $DMSP_p$, and Ehux whereas abundance of attached bacteria was positively correlated with TEP and POC. The negative correlation between TEP, on one hand, and csBPP and abundance of attached bacteria, on the other hand, indicates that TEP -due to its sticking properties- may be efficient in scavenging bacteria from the surrounding water but a poor bacterial substrate.

For dissolved organic matter and primary production (Table 2b) the analysis revealed that BPP of free-living and attached bacteria was positively correlated to DMS, $DMSP_d$, and PrProd but in a varying order. PrProd most strongly correlated with csBPP of free-living and attached bacteria. CsBPP of free-living bacteria was also positively related to DMS whereas csBPP of attached bacteria was negatively related to DOC. Abundance of both free-living and attached bacteria, however, was closely correlated to $DMSP_d$, DMS, and DOC but in a varying order.

Table 2. Results of stepwise multiple regression analysis. Parameters correlated to **(A)** particulates (POC, C:N, TEP, $DMSP_p$, Chl-*a*, Ehux, Diatoms, Cyano), **(B)** dissolved organic matter and primary production (DOC, DMS, $DMSP_d$, PrProd), and **(C)** virus (Virus, Big Virus). For abbreviations and n see legend Table 1.

	BPP free	BPP attached	csBPP free	csBPP attached	Bacteria free	Bacteria attached
(A)	F=272.118, <0.001 parameter,T-, p-value $DMSP_p$, 16.496, <0.001	F=48.232, <0.001 parameter,T-, p-value $DMSP_p$, 11.453, <0.001 TEP, –5.172, <0.001 C:N, 2.075, <0.041	F=52,006, <0.001 parameter,T-, p-value Ehux, 7.211, <0.001	F=37.004, <0.001 parameter,T-, p-value Cyano, -3.539, 0.001 TEP, –6.522, <0.001 $DMSP_p$, 3.532, 0.001	F=89.150, <0.001 parameter,T-, p-value POC, 3.436, 0.001 Cyano, 5.362, <0.001 $DMSP_p$, 4.962, <0.001 Ehux, 3.551, 0.001	F=109.739, <0.001 parameter,T-, p-value TEP, 5.644, <0.001 POC, 3.442, 0.001
(B)	F=81.083, <0.001 parameter,T-, p-value DMS, 8.219, <0.001 $DMSP_d$, 5.739, <0.001 PrProd, 4.091, <0.001	F=79.114, <0.001 parameter,T-, p-value PrProd, 9.344, <0.001 DMA, 5.896, <0.001 $DMSP_d$, 3.451, 0.001	F=85.915, <0.001 parameter,T-, p-value PrProd, 10.957, <0.001 DMS, 3.177, 0.002	F=46.075, <0.001 parameter,T-, p-value PrProd, 5.725, <0.001 DOC, –3.864, <0.001	F=29.375, <0.001 parameter,T-, p-value $DMSP_d$, 4.463, <0.001 DMS, 4.826, <0.001 DOC, 4.381, 0.001	F=41.772, <0.001 parameter,T-, p-value DMS, 8.217, <0.001 DOC, 5.972, <0.001 $DMSP_d$, 2.292, 0.025
(C)	F=81.734, <0.001 parameter,T-, p-value Big Virus, -9.041, <0.001	F=158.281, <0.001 parameter,T-, p-value Big Virus, -12.581, <0.001	F=47.048, <0.001 parameter,T-, p-value Big Virus, -5.261, <0.001 Virus, -2.434, 0.017	F=61.984, <0.001 parameter,T-, p-value Virus, -7.873, <0.001	F=31.473, <0.001 parameter,T-, p-value Big Virus, -7.365, <0.001 Virus, 7.158, <0.001	F=44.143, <0.001 parameter,T-, p-value Big Virus, -9.270, <0.001 Virus, 7.408, <0.001

The stepwise multiple regression analysis for virus revealed a negative relationship between the abundance of big virus and most bacterial parameters (BPP and abundance of free-living and attached bacteria and csBPP of free-living bacteria). Interestingly, csBPP of free-living and attached bacteria were negatively but abundances of both free-living and attached bacteria positively correlated to total virus. To get a better estimate on virus production we have estimated viral production by $n_t - n_{t-1}$ (whereby n_t=viral abundance at a given time point and n_{t-1}=viral abundance 1 day before sampling time point) and specific viral production by $(n_t\text{-}n_{t-1})/(n_t+n_{t-1})/2$. Our estimates revealed that solely numbers of free-living and attached bacteria were positively correlated with viral production and even better with specific viral production. In contrast, the production of big virus was negatively correlated with csBPP of free-living and attached bacteria but not with their abundance. This suggests that the role of virus in controlling bacterial dynamics can be contrary. In addition to bacteriophages, Larsen et al. (2008) found several phytoplankton viruses in the present experiment. Preferential lysis of algal cells may result in release of phytoplanktonic DOM and, hence, serves as an important DOM source for bacteria.

To further test for dependency on pCO_2 we have performed the CHOW test with univariate GLM (Table 3). Solely, linear regressions between BPP of free-living bacteria, BPP of attached bacteria or csBPP of attached bacteria and the C:N ratio of suspended matter revealed a significant effect of pCO_2.

3.5 Molecular characterization of free-living and particle-associated bacterial communities

Structural diversity of bacterial communities was investigated by DGGE analyses of partial 16S rRNA gene fragments. DGGE analyses were performed for free-living and

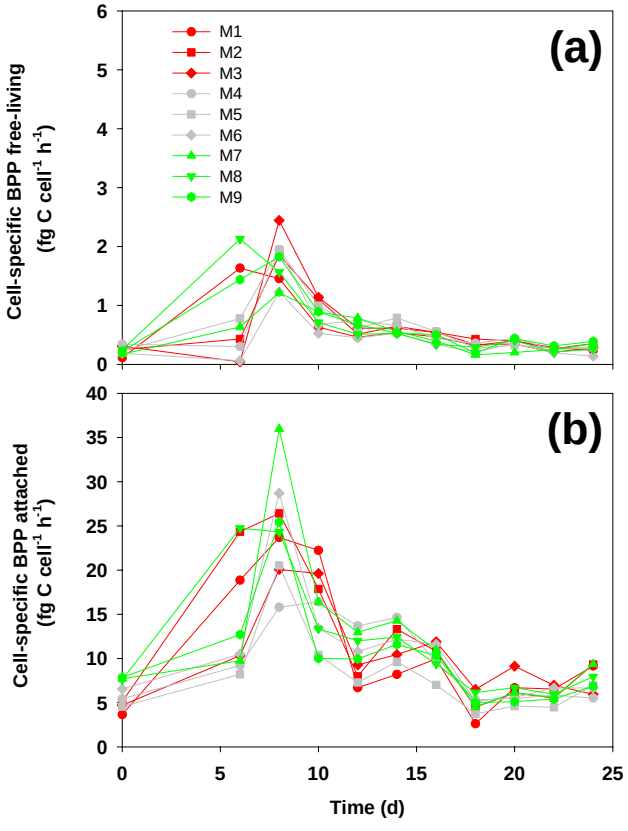

Fig. 3. Cell-specific BPP of **(a)** free-living ($\leq$5.0 μm$\geq$0.2 μm) and **(b)** attached bacteria ($\geq$5.0 μm). M1–M3 mesocosms with 3×CO_2, M4–M6 mesocosms with 2×CO_2, and M7–M9 mesocosms with 1×CO_2.

Table 3. CHOW test with univariate GLM to test for dependencies on pCO_2. For abbreviations see legend Table 1. n=87.

Parameter	BPP free	BPP attached	csBPP free	csBPP attached
C:N	intercept	intercept	ns	intercept
	p=0.004	p=0.003		p=0.027
	F=5.923	F=6.432		F=3.762
	slope	slope		slope
	p=0.004	p=0.003		p=0.034
	F=5.819	F=6.407		F=3.526
	dF=2	dF=2		dF=2

particle-associated bacteria separately to obtain higher phylogenetic resolution and to receive closer information on potential responses of bacterial communities to differences in CO_2 concentrations. Investigation of bacterial community structure was conducted for mesocoms M2 ($3\times CO_2$), M5 ($2\times CO_2$), and M8 ($1\times CO_2$), each representing one of the three different pCO_2 treatments. Samples were taken in intervals of 4 to 6 days from the beginning (day zero, T0) to the end (day 24, T24) of the experiment. In all mesocosms both free-living and particle-associated bacteria showed a relatively high phylogenetic diversity in respect to absolute numbers of DGGE bands. Numbers of DGGE bands varied between 11 and 21 (mean 15±2.7) and between 12 and 25 (mean 17±3.3) for free-living and particle-associated bacteria, respectively. Even though free-living and particle-associated bacteria showed similar numbers of DGGE bands, distinct differences occurred in their respective banding patterns (Fig. 4). However, as determined by ANOSIM of the DGGE banding patterns differences between free-living and particle-associated bacteria communities were significant only within mesocosm M5 ($p\leq0.001$). Differences between the two bacterial fractions in mesocosms M2 and M8 were not statistically significant ($p\geq0.05$).

As indicated by cluster analyses of DGGE banding patterns and ANOSIM community composition of free-living bacteria significantly differed between mesocosms (Fig. 4, Table 4). In contrast, cluster analyses of particle-associated bacteria did not reveal any clustering between samples of the three mesocosms (Fig. 4) and no significant differences between mesocosms were observed by ANOSIM (Table 4).

Cluster analyses of particle-associated bacteria, however, indicate temporal clusters which can be directly related to phytoplankton bloom development (Fig. 4). Three major clusters (Cluster 1 to 3) were identified, representing (a) initiation (T0) and end of the experiment (T24), (b) phytoplankton bloom increase (T6) and decline (T18), and (c) maximum of the phytoplankton bloom (T10 and T14), respectively. DGGE banding patterns of both free-living and particle-associated bacteria from the fjord formed distinct clusters which were clearly separated from those in the mesocosms (Fig. 4).

NMS analyses of DGGE banding patterns support the results of our ANOSIM analyses and reveal rather distinct populations of free-living bacteria (Fig. 5A) but highly intermixed populations of particle-associated bacteria (Fig. 5B) at different pCO_2 levels. In both bacterial fractions the samples from the fjord formed a narrow cluster which, especially for particle-associated bacteria, was different from those in the mesocosms. Samples M2-T6 and M5-T18 of the free-living bacteria were exceptional in their position in the NMS ordination plot which may have been the result of their very weak banding pattern.

3.6 Phylogenetic analyses of sequenced DGGE bands

Sequencing and phylogenetic characterization of selected DGGE bands indicated the occurrence of *α-proteobacteria*, *γ-proteobacteria*, *Bacteroidetes*, and *Actinobacteria* in the three investigated mesocosms. We also detected several sequences originating from chloroplasts of *Emiliania huxley*, uncultured diatoms, and members of the phylum *Prasinophyta* (Fig. 6). Except for the single actinobacterial sequence belonging to freshwater *Actinobacteria*, all other sequences were phylogenetically affiliated to marine bacterial clusters. No distinct differences in bacterial community composition were observed on the phylogenetic level between the three mesocosms in respect to different pCO_2 concentration and phytoplankton bloom development. We also did not observe any distinct phylogenetic differences between free-living and particle-associated bacteria. Sequences of free-living and particle-associated bacteria were distributed equally throughout the constructed phylogenetic tree without indicating formation of fraction-specific clusters (Fig. 6).

4 Discussion

4.1 Dependency of microbial dynamics on pCO_2

In a previous mesocosm study using a similar experimental set up Grossart et al. (2006b) found that growth rate and BPP of heterotrophic bacteria were highest at highest pCO_2 whereas bacterial abundance remained similar for most time of the experiment. Although mean ectoenzymatic activities (protease, α- and β-glucosidase) were also increased at higher pCO_2, pCO_2 dependency was statistically significant only for protease activity. In contrast to our present study, algal dynamics in the former study was strongly dependent on pCO_2 suggesting that changes in bacterial activities were mainly correlated to pCO_2 induced changes in phytoplankton growth and community composition. In the present study, however, neither bacterial abundance nor BPP were different among pCO_2 treatments. Solely, linear regressions between BPP of free-living bacteria, BPP of attached bacteria or csBPP of attached bacteria and C:N ratio of suspended matter were significantly different between pCO_2 levels (Table 3). The effects are not consistently strong enough to re-

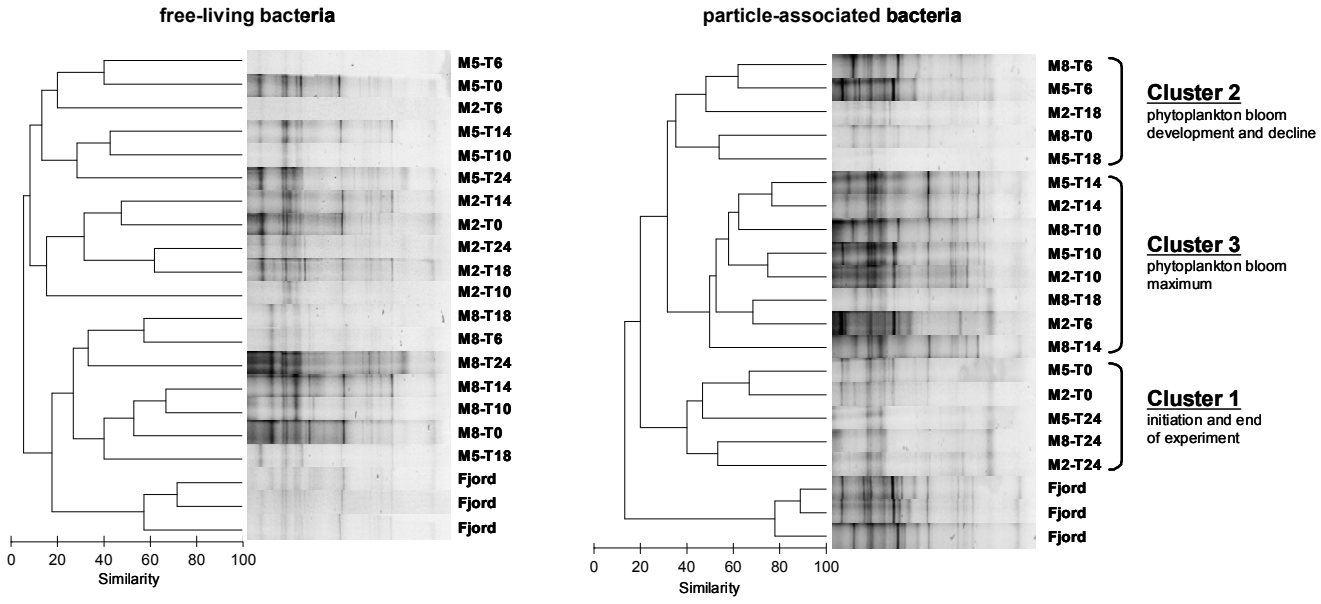

Fig. 4. Cluster analyses including the corresponding DGGE profiles of PCR-amplified 16S rRNA gene fragments of free-living and particle-associated bacterial communities of the mesocosm M2 ($3\times CO_2$), M5 ($2\times CO_2$), and M8 ($1\times CO_2$). Sample identification numbers indicate mesocosm and date of each sample. Samples designated with "Fjord" are water samples originating from the Fjord outside of the mesocosms which were used as external standard on each DGGE gel for comparison of the DGGE profiles across different gels.

Table 4. Comparison of DGGE banding patterns of free-living and particle-associated bacteria of mesocosms M2 ($3\times CO_2$), M5 ($2\times CO_2$), and M8 ($1\times CO_2$) by using ANOSIM statistics.

free-living bacteria	Sample Statistic (R)	Significance level (p)
M2 vs. M5	0.487	0.002
M2 vs. M8	0.395	0.002
M5 vs. M8	0.525	0.002
particle-associated bacteria		
M2 vs. M5	–0.089	0.85
M2 vs. M8	0.016	0.417
M5 vs. M8	0.074	0.224

The global tests revealed sample statistics of 0.468 for free-living bacteria and 0.452 for particle-associated bacteria with significance values of p 0.001 and p 0.453, respectively.

veal significant differences of the parameters between different pCO_2 levels. However, differently shaped relations between bacterial production parameters and C:N at different pCO_2 levels may indicate different underlying mechanisms. For example, the C:N ratios of the suspended particulate organic matter in the upper water layer may have been largely dominated by living algal biomass leading to a rather constant C:N ratio in all treatments. A higher loss of organic carbon from the upper layer of the stratified mesocosms at higher pCO_2 has been previously shown (Engel, 2002; Engel et al., 2004) and has been assigned to higher concentrations of TEP at higher pCO_2. Higher abundances of TEP provide larger surfaces for bacterial attachment which may result in higher bacterial activities (Grossart et al., 2007), and promote aggregation and loss of C-rich particulate organic matter (Passow, 2002). In our study, the stoichiometry of carbon to nitrogen drawdown (C:N) increased from a value of 6.0 under present pCO_2 to 8.1 at high pCO_2 (Riebesell et al., 2007) which may indicate pCO_2-dependent changes in carbon and/or nitrogen consumption by heterotrophic bacteria, especially of attached bacteria.

Our stepwise multiple regression analysis revealed that TEP positively correlated with abundance of attached bacteria but negatively with their csBPP. Due to their sticking properties TEP can efficiently scavenge bacteria but may lower csBPP of attached bacteria because of their low

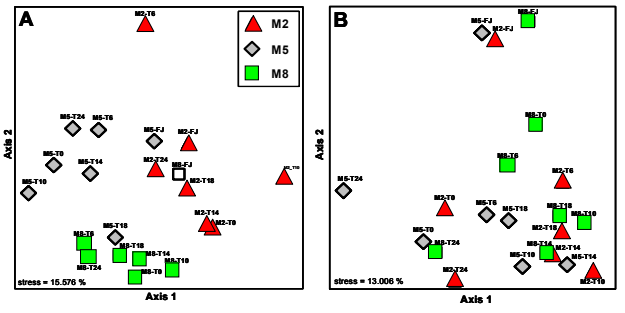

Fig. 5. NMS ordination plots of DGGE banding patterns of **(A)** free-living ($\leq$5.0$\geq$0.2 μm) and **(B)** particle-associated bacteria ($\geq$5.0 μm).

nitrogen and phosphorus content (Passow, 2002). In addition, a pCO_2 dependent algal carbon consumption may result in increased phytoplankton exudation (e.g. Obernosterer and Herndl, 1995; Biddanda and Benner, 1997) with high proportions of carbon rich DOM which is less accessible to microbial degradation (Søndergaard et al., 2000; Thingstad et al., 1997). Since the drawdown of nutrients and phytoplankton community composition were similar in all mesocosms (Riebesell et al., 2007), we conclude that in addition to nutrient regime and phytoplankton community composition (Conan et al., 2007) carbon availability can greatly affect production and composition of new DOM. If so, an increasing pCO_2 in the upper ocean must have profound implications for microbial utilization of the oceanic DOM pool. In our experiment, DOC and BPP as well as csBPP of both free-living and attached bacteria were negatively correlated which indicates that increasing concentrations of DOC throughout the bloom do not necessarily stimulate bacteria secondary production. As indicated by Tanaka et al. (2008) after the peak of the phytoplankton bloom the released labile DOC may have been rich in carbon such as glucose whereas P and N were depleted. This suggests that there is a slight but rather indirect effect of changes in pCO_2 on bacterial activities and community structure that is mainly related to phytoplankton carbon consumption, DOC exudation, as well as TEP formation and subsequent sedimentation (also see Tanaka et al., 2008).

We are aware of the fact that the sudden increase in pCO_2 levels does not reflect natural conditions where a more steady increase in pCO_2 levels over longer time spans occurs. Hence, in the present study all organisms, especially at higher trophic levels, had rather little time to physiologically adapt to the new environmental conditions.

4.2 Coupling of heterotrophic bacteria to phytoplankton bloom development

Abundance and BPP of both free-living and attached bacteria were tightly coupled to phytoplankton bloom development and did not show any significant differences between the treatments. The relatively high bacterial abundance at the beginning of the experiment, in particular of free-living bacteria, may have been caused by addition of freshwater to the upper water layers of each mesocosm, disruption of jelly fish during mesocosm filling, and bubbling. When excluding the initial phase of the mesocosm experiment, abundance of free-living bacteria increased from day 6 on and peaked during the decline of the algal bloom whereas the second increase in numbers of free-living bacteria occurred in parallel to an increase in dinoflagellates and unicellular cyanobacteria towards the end of the experiment. In contrast, the abundance of attached bacteria exhibited only one peak which occurred slightly earlier than the first peak of free-living bacteria and in parallel to phytoplankton development (Schulz et al., 2008). Numbers of attached bacteria were much lower than those of free-living bacteria. In a previous study (Grossart et al., 2006b) we also found that maxima in abundance of free-living bacteria surpassed that of attached bacteria by ca. 10-fold. Interestingly, numbers of free-living bacteria in the present study dramatically dropped several days before the phytoplankton bloom had reached its maximum. At the same time viral numbers and estimated production greatly increased (Larsen et al., 2008) suggesting viral lysis of free-living bacteria. In contrast, attached bacteria continuously increased during the second half of the bloom and even during the declining phase. Since there were no pronounced differences in phytoplankton and bacterial dynamics between the different treatments of the present study, we conclude that coupling between phytoplankton and heterotrophic bacteria was similar for all mesocosms.

In contrast to abundance, BPP of free-living and attached bacteria were in the same range and highest during the peak and the decline of the phytoplankton bloom. Whereas BPP of attached bacteria dramatically increased at the peak of the bloom and remained high during the breakdown of the bloom, BPP of free-living bacteria strongly increased after the phytoplankton bloom and reached its maximum when phytoplankton biomass was low but POC, PON, and POP still high (Schulz et al., 2008). High exoenzymatic activities of attached bacteria on senescent diatom cells leading to a subsequent increase in dissolved DOM have been recently found (Grossart et al., 2005). Other studies (e.g. Smith et al., 1992; 1995) show that high exoenzymatic activities on marine snow lead to an increasing release of DOM into the surrounding water which stimulates growth of free-living bacteria. Since the dynamics of free-living bacteria followed that of attached bacteria, a similar scenario seems to be likely for the present study. CsBPP of both bacterial fractions, however, reached its maximum at the high of the algal bloom

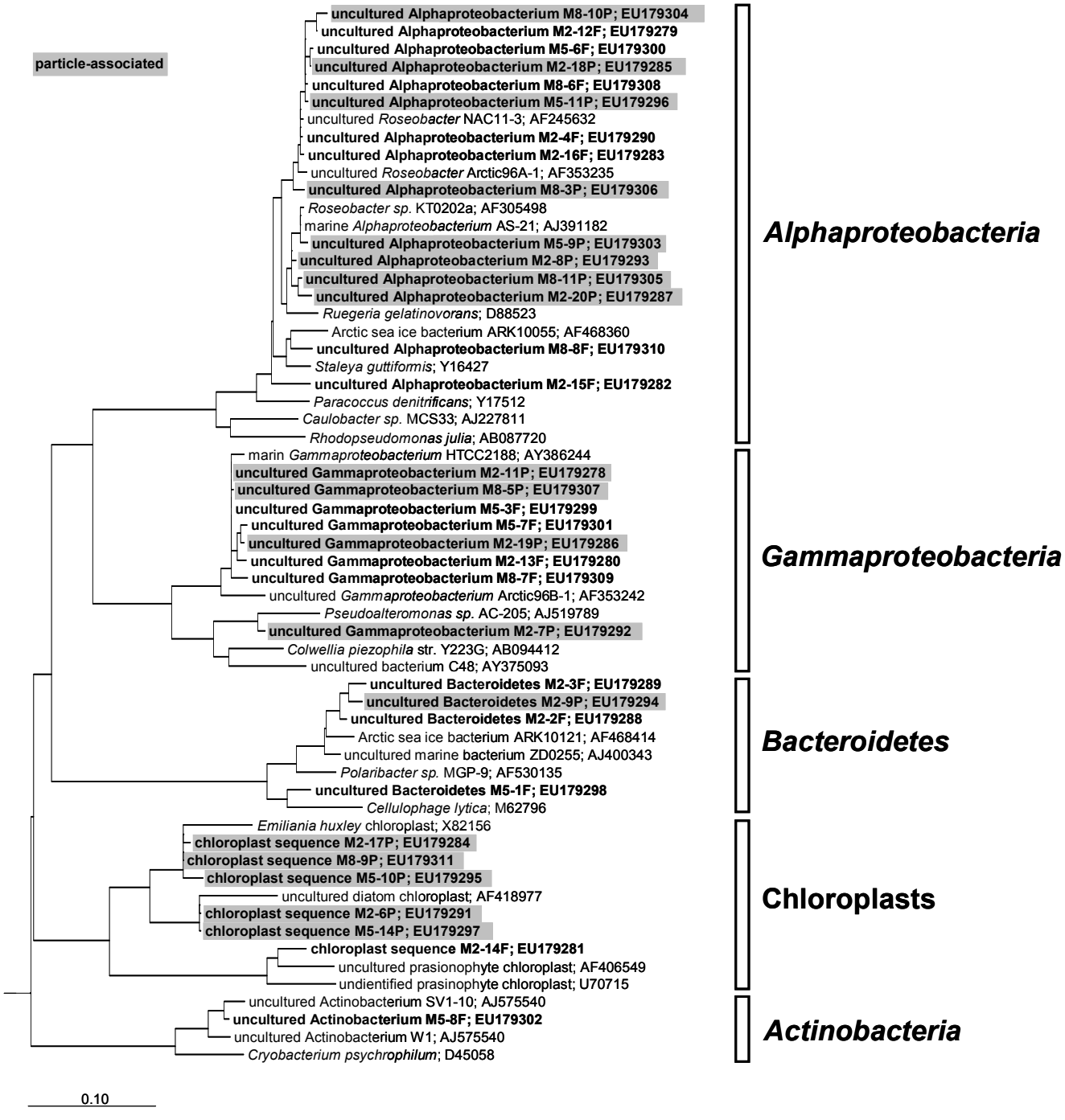

Fig. 6. Maximum Likelihood tree of 16S rRNA gene sequences of free-living and particle-associated bacteria derived from DGGE bands of the three mesocosms M2 ($3\times CO_2$), M5 ($2\times CO_2$), and M8 ($1\times CO_2$). Sequences of this study are shown in bold letters. Sequences of particle-associated bacteria are additionally marked by grey boxes. GenBank accession numbers are given. The sequence identification number indicates from which mesocosm the sequences are derived (e.g. M2-X, M5-X, or M8-X). The scale bar corresponds to 10% base substitutions.

indicating a tight coupling between bacteria activity and phytoplankton development, especially when P and N were depleted in the ambient water (Tanaka et al., 2008). The much higher csBPP of attached than of free-living bacteria may indicate a closer and more efficient coupling of phytoplankton-associated bacteria presumably due to a lower spatial distance between algae and bacteria and a higher availability of nutrients. In addition, our statistics (Table 3a and b) shows that indeed both bacterial fractions were tightly coupled to algal parameters but in a different manner. Surprisingly, BPP of free-living bacteria was negatively correlated with diatoms, whereas csBPP of attached bacteria was negatively correlated with Cyano and TEP. In contrast, both csBPP of free-living and attached bacteria positively correlated with Ehux. Hence, the presence of different algal species leads to differences in the correlation between free-living and attached bacteria to phytoplankton bloom development. This notion points to differences in the functional role of free-living vs. attached bacteria for oceanic nutrient and energy cycling (Simon et al., 2002).

Another important point is that free-living and attached bacteria at certain times may have experienced great differences in the availability of limiting nutrients, such as phophorus and nitrogen (Tanaka et al., 2008). It has been suggested by Thingstad et al. (2005) that specific bacteria, such as *Vibrio splendidus*, obtain a competitive advantage for mineral nutrients by using a non-limiting carbon source to increase their size, without thereby increasing their cellular quota of the limiting element. According to these authors the benefit would be threefold: 1) increased affinity, 2) decreased predation pressure, and 3) storage of energy and carbon for potential later use under C-limited conditions. The specific environment required for such a beneficial strategy would be access to a pool of assimilable organic C in excess of that required for growth. Similar conditions are given for bacteria clustering in the vicinity or being attached to phytoplankton cells and organic matter aggregates where a substantial release of C rich organic matter due to phytoplankton exudation or by bacterial ectoenzymatic activities has been observed (Kiørboe and Jackson 2001; Grossart et al., 2006a; Grossart et al., 2007). An increase in organic matter and nutrient supply once a bacterium stays in the vicinity or has attached to a larger particle has been previously calculated by Kiørboe and Jackson (2001). In our study mainly members of the *Roseobacter* clade and of γ*-Proteobacteria* seem to follow the above mentioned strategy (see also bellow).

4.3 Cycling of $DMSP_{d+p}$ and DMS

Abundance and BPP of both free-living and attached bacteria correlate well with the concentration of $DMSP_d$ and especially $DMSP_p$ (Tables 1, 2a and b). This also points to a tight coupling between bacteria and phytoplankton dynamics. $DMSP_p$ is produced in some phytoplankton groups (Keller et al., 1989) as an osmolyte (e.g. Dickson and Kirst, 1986), cryoprotectant (Karsten et al., 1996), as an antioxidant (Sunda et al., 2002) or overflow mechanism (Stefels, 2000). Most $DMSP_p$ is transferred to the dissolved phase ($DMSP_d$) upon demise of phytoplanktonic cells through grazing, autolysis, and viral lysis (Stefels et al., 2007). There, $DMSP_d$ is available for bacterial degradation and may serve as an important substrate and energy source for marine bacteria (Kiene and Linn, 2000). Furthermore, marine bacteria can satisfy almost all their sulphur demand through DMSP consumption (e.g. Kiene et al., 2000). By using a combination of microautoradiography and CARD-FISH Vila-Costa and coworkers (2007b) showed that members of α*-proteobacteria* (Roseobacter and SAR11) and γ*-proteobacteria* accounted for most of the bacterial DMSP-S assimilating cells during a seasonal cycle in the Mediterranean. These two groups are the major bacterial groups found in the present study (see below). The most common pathway of DMSP consumption, however, is the demethylation/demethiolation pathway, which drives DMSP away from DMS production.

A Lagrangian study of a coccolithophore bloom in the North Sea revealed that microzooplankton grazing can account for the majority of $DMSP_p$ degradation (Archer et al., 2003). In addition, viruses have been implicated in the collapse of blooms of *E. huxleyi* (Wilson et al., 2002), which was also the case in our study (Larsen et al., 2008). In a more recent study, however, Evans et al. (2007) found that for *E. huxleyi* microzooplankton grazing is more important for DMS production than viral lysis – most likely because virally infected cells have lower lyases activities. Unfortunately, we do not have enough data on microzooplankton grazing to study its relevance for DMS production.

In the North Sea, Zubkov et al. (2001) found that free-living bacteria of the genus *Roseobacter* are actively involved into the pelagic sulphur cycling via degradation of $DMSP_d$. In our study, this genus comprised a major fraction of α*-proteobacteria*, both free-living and attached and BPP and abundance of both bacterial fractions correlated well with $DMSP_d$ and even better with $DMSP_p$. This suggests that these bacteria, either free-living or attached, are involved in DMSP cycling.

CsBPP of both bacterial fractions was most strongly correlated to primary production and only csBPP of free-living bacteria was also positively coupled to DMS. DMS is a climatically active trace gas (Charlson et al., 1987) and is primarily formed in seawater by interactions of the microbial food web (Simó et al., 2002). DMS concentrations in seawater are the result of a complex web of production and loss processes (Simó et al., 2002). In particular, bacterial processes are central in controlling dissolved DMS concentrations (Vila-Costa et al., 2007a; Howard et al., 2006; Kiene et al., 2000). DMS is formed when DMSP is cleaved by a group of isozymes, which are produced in the microbial community by phytoplankton species such as *E. huxleyi*, *Phaeocystsis* species and some dinoflagellates (Steinke et al., 1998;

2002; Stefels et al., 1995) and by some bacteria (Ledyard and Dacey, 1994; Todd et al., 2007). Kiene et al. (2000) suggests that the bacterial yield of DMS from DMSP consumption depends upon bacterial sulphur demand and DMSP concentration. Besides photolysis bacterial degradation is the dominant loss process for DMS in the ocean (e.g. Kiene and Bates, 1990). Whereas most marine bacteria can assimilate DMSP (generalists), it has been suggested that DMS degraders are specialists, comprising approximately 33% of the bacterial community (Vila-Costa et al., 2007a).

The correlation of csBPP of free-living bacteria to DMS concentration in our study (Table 2b) implies that free-living bacteria participated in DMS consumption. Vila-Costa et al. (2007a) found that not only bacteria of the *Methylophaga* group are prolific DMS consumers, but also that members of the *Roseobacter* group are able to assimilate DMS to a certain extent. In our study, members of the *Roseobacter* group formed several dominant DGGE bands whereas members of the *Methylophaga* group were not found (see below).

4.4 Community composition and phylogeny

Although differences in DGGE banding patterns of free-living and attached bacteria were minor, temporal succession of both bacterial fractions was different. Whereas free-living bacteria formed distinct clusters among the different treatments throughout the whole study period, temporal dynamics of attached bacteria closely followed that of phytoplankton development. This was not reflected by our 16S rRNA gene based phylogeny of the excised DGGE bands which revealed that the majority of free-living as well as attached bacteria belonged to similar groups of the α- and γ-*proteobacteria*, and Bacteroidetes. α-*proteobacteria*, mainly of the *Roseobacter* group, γ-*proteobacteria*, in particular of the *Pseudoaltermonas* group, and specific *Bacteroidetes* have been frequently found to be associated to various phytoplankton species of different phylogenetic groups in laboratory cultures and in the sea (Grossart et al., 2005; Garces et al., 2007 and references therein). Whereas Grossart et al. (2005) found significant differences between free-living and attached bacterial communities in laboratory diatom cultures, differences between the two bacterial fractions in the present study were less obvious. Both *Roseobacter* and *Pseudoaltermonads* are highly motile and it has been shown that some *Roseobacter* species express high chemotaxis in the presence of organic matter such as marine broth and DMSP (Kiørboe et al., 2002). Furthermore, quorum sensing via acylated homoserine lactones (AHLs) seems to be a common feature of *Roseobacter* species (Gram et al., 2002; Martens et al., 2007). In addition to their blooming during phytoplankton blooms, *Roseobacter* and presumably *Pseudoalteromonas* and *Bacteroidetes* seem to be well adapted to rapidly respond to phytoplankton development. It may be difficult to distinguish between free-living and attached bacterial communities since many chemotactic species show frequent attachment and subsequent detachment (Kiørboe et al., 2002). Our results suggest that bacterial community analysis, solely based on the 16S rRNA gene, can provide valuable results on the interaction between heterotrophic bacteria and phytoplankton development and, hence, the functioning of the microbial food web.

5 Summary

Microbial dynamics in our mesocosm plankton communities was correlated with phytoplankton development. Changes in pCO_2 led to significant changes in community structure of free-living but not of attached bacteria which were more tightly correlated to phytoplankton dynamics. Statistical analysis solely revealed a pCO_2 dependency for linear regressions between C:N ratio of suspended matter and BPP of free-living and attached bacteria as well as csBPP of attached bacteria. The differently shaped relations between bacterial production parameters and C:N at different pCO_2 levels may indicate different underlying mechanisms. Our results provide some indication that pCO_2 induced changes in phytoplankton carbon fixation and community succession will have an impact on microbial energy consumption and carbon as well as sulphur cycling due to the rather tight coupling between phytoplankton and microbial dynamics in the pelagic ocean. In particular, chemotactic and attached bacteria may greatly benefit from a tight coupling to phytoplankton cells and organic aggregates since by doing so they may have a competitive advantage not only for organic carbon but also for mineral nutrients. Slight changes in organic matter cycling due to differences in pCO_2 may be hard to detect in short-term mesocosm experiments but may accumulate in the long-term. Hence, we suggest that further studies on pCO_2 induced changes on microbial activities should take a longer time scale into account.

Acknowledgements. We would like to thank all participants of the PeECE III mesocosm experiment (http://peece.ifm-geomar.de) for their valuable technical assistance, data acquisition, and many fruitful discussions. The staff at the Marine Biological Station, University of Bergen, in particular Tomas Sørlie and Agnes Aadnesen, and the Bergen Marine Research infrastructure (RI) are gratefully ackowledged for support in mesocosm logistics. M. Steinke and S. Turner are thanked for assistance in DMS/DMSP measurements and numerous discussions. Kirsten Pohlmann is warmly acknowledged for help in statistical analyses and her comments on this manuscript. This work was supported by a grant of the German Science Foundation given to H.P.G. (GR 1540/8-2) and a grant of the German National Academic Foundation given to M.A.

Edited by: J.-P. Gattuso

References

Allgaier, M. and Grossart, H.-P.: Diversity and seasonal dynamics of Actinobacteria in four lakes in Northeastern Germany, Appl. Environ. Microbiol., 72, 3489–3497, 2006a.

Allgaier, M. and Grossart, H.-P.: Seasonal dynamics and phylogenetic diversity of free-living and particle-associated bacterial communities in four lakes in northeastern Germany, Aquat. Microb. Ecol., 45, 115–128, 2006b.

Archer, S. D., Stelfox-Widdicombe, C. E., Malin, G., and Burkill, P. H.: Is dimethyl sulphide production related to microzooplankton herbivory in the southern North Sea?, J. Plankton Res., 25, 235–242, 2003.

Armstrong, R. A., Lee, C., Hedges, J. I., Honjo, S., and Wakeham, S. G.: A new, mechanistic model for organic carbon fluxes in the ocean based on the quantitative association of POC with ballast minerals, Deep-Sea Res. II, 49, 219–236, 2002.

Biddanda B. and Benner, R.: Carbon, nitrogen, and carbohydrate fluxes during the production of particulate and dissolved organic matter by marine phytoplankton, Limnol. Oceanogr., 42, 506–518, 1997.

Burkhardt, S., Amoroso, G., Riebesell, U., and Sultemeyer, D.: CO_2 and HCO_3^- uptake in marine diatoms acclimated to different CO_2 concentrations, Limnol. Oceanogr., 46, 1378–1391, 2001.

Caldeira, K. and Wickett, M. E.: Anthropogenic carbon and ocean pH, Nature, 425, 365, 2003.

Charlson, R. J., Lovelock, J. E., Andreae, M. O., and Warren, S. G.: Oceanic phytoplankton, atmospheric sulphur, cloud albedo and climate, Nature, 326, 655–661, 1987.

Clarke, K. R. and Green, R. H.: Statistical design and analysis for a "biological effects" study, Mar. Ecol. Progr. Ser., 46, 213–226, 1988.

Clarke, K. R. and Gorley, R. N.: PRIMER v5: User manual/tutorial, PRIMER-E, Plymouth UK, 91 pp., 2001.

Conan, P., Søndergaard, M., Kragh, T., Thingstad, F., Pujo-Pay, M., Williams, P. J. le B., Markager, S., Cauwet, G., Borch, N. H., Evan, D., and Riemann, B.: Partitioning of organic production in marine plankton communities: The effects of inorganic nutrient ratios and community composition on new dissolved organic matter, Limnol. Oceanogr., 52, 753–765, 2007.

Dickson, D. M .J. and Kirst, G. O.: The role of b-dimethylsulfoniopropionate, glycine betaine and homarine in the osmoacclimation of *Platymonas subcordiformis*, Planta 167, 536–543, 1986.

Egge, J. K., Thingstad, T. F., Engel, A., Bellerby, R. G. J., and Riebesell, U.: Primary production during nutrient-induced blooms at elevated CO_2 concentrations, Biogeosciences Discuss., 4, 4385–4410, 2007, http://www.biogeosciences-discuss.net/4/4385/2007/.

Engel, A.: Direct relationship between CO_2 uptake and transparent exopolymer particle production in natural phytoplankton, J. Plankton Res., 24, 49–53, 2002.

Engel, A., Thoms, S., Riebesell, U., Rochelle-Newall, E., and Zondervan, I.: Polysaccharide aggregation as a potential sink of marine dissolved organic carbon, Nature, 428(6986), 929–932, 2004.

Engel, A., Zondervan, I., Aerts, K., Beaufort, L., Benthien, A., Chou, L., Delille, B., Gattuso, J. P., Harlay, J., Heemann, C., Hoffman, L., Jacquet, S., Nejstgaard, J., Pizay, M.-D., Rochelle-Newall, E., Schneider, U., Terbrueggen, A., and Riebesell, U.: Testing the direct effect of CO_2 concentration on a bloom of the coccolithophorid *Emiliania huxleyi* in mesocosm experiments, Limnol. Oceanogr., 50, 493–507, 2005.

Evans, C., Kadner, S. V., Darroch, L. J., Wilson, W. H., Liss, P. S., and Malin, G.: The relative significance of viral lysis and microzooplankton grazing as pathways of dimethylsulfoniopropionate (DMSP) cleavage: An *Emiliania huxleyi* culture study, Limnol. Oceanogr., 53, 1036–1045, 2007.

Fry, B., Hopkinson, C. S., Nolin, A., and Zweifel, U. L.: Long-term decomposition of DOC from experimental diatom blooms, Limnol. Oceanogr., 41, 1344–1347, 1996.

Garces, E., Vila, M., Rene, A., Alonso-Saez, A. S., Luglie, A., Maso, M., and Gasol, J. M.: Natural bacterioplankton assemblages composition during blooms of Alexandrium spp. (Dinophyceae) in NW Mediterranean coastal waters, Aquat. Microb. Ecol., 46, 55–70, 2007.

Gram, L., Grossart, H.-P., Schlingloff, A., and Kiørboe, T.: Production of acylated homoserine lactones by *Roseobacter* strains isolated from marine snow, Appl. Eviron. Microbiol., 68, 4111–4116, 2002.

Grossart, H.-P. and Ploug, H.: Microbial Degradation of Organic Carbon and Nitrogen on Diatom Aggregates, Limnol. Oceanogr., 46, 267–277, 2001.

Grossart, H.-P., Levold, F., Allgaier, M., Simon, M., and Brinkhoff, T.: Marine diatom species harbour distinct bacterial communities, Environ. Microbiol., 7, 860–873, 2005.

Grossart, H.-P., Czub, G., and Simon, M.: Specific interactions of planktonic algae and bacteria: Implications for aggregation and organic matter cycling in the sea, Environ. Microbiol., 8, 1074–1084, 2006a.

Grossart, H.-P., Allgaier, M., Passow, U., and Riebesell, U.: Testing the effect of CO_2 concentration on dynamics of marine heterotrophic bacteriaoplankton, Limnol. Oceanogr., 51, 1–11, 2006b.

Grossart, H.-P., Tang, K. W., Kiørboe, T., and Ploug, H.: Comparison of cell-specific activity between free-living and attached bacteria using isolates and natural assemblages, FEMS Microbiol. Lett., 266, 194–200, 2007.

Hoppe, H. G., Ducklow, H., and Karrasch, B.: Evidence for dependency of bacterial-growth on enzymatic hydrolysis of particulate organic matter in the mesopelagic ocean, Mar. Ecol. Prog. Ser., 93(3), 277–283, 1993.

Howard, E. C., Henriksen, J. R., Buchan, A., Reisch, C. R., Buergmann, H., Welsh, R., Ye, W. Y., Gonzalez, J. M., Mace, K., Joye, S. B., Kiene, R. P., Whitman, W. B., Moran, M. A.: Bacterial taxa that limit sulfur flux from the ocean, Science, 314, 649–652, 2006.

Karsten, U., Kück, K., Vogt, C., Kirst, G. O.: Dimethylsulfoniopropionate production in phototrophic organisms and its physiological function as a cryoprotectant. In: Kiene, R.P., Visscher, P.T., Keller, M.D., Kirst, G.O. (Eds.). Biological and Environmental Chemistry of DMSP and Related Sulfonium Compounds, Plenum Press, New York, 143–153, 1996.

Keller, M. D., Bellows, W. K. And Guillard, R. R. L.: Dimethyl sulphide production in marine phytoplankton. ACS Symposium Series, 393, 167–182, 1989.

Kiene, R. P. and Bates, T. S.: Biological removal of dimethylsulfide from sea water. Nature, 345, 702–705, 1990.

Kiene, R. P., Linn, L. J., and Bruton, J. A.: New and important

roles for DMSP in marine microbial communities. J. Sea Res., 43, 209–224, 2000.

Kiene, R. P. and Linn, L. J.: Distribution and turnover of dissolved DMSP and its relationship with bacterial production and dimethylsulfide in the Gulf of Mexico, Limnol. Oceanogr., 45, 849–861, 2000.

Kiørboe, T. and Jackson G. A. Marine snow, organic solute plumes, and optimal chemosensory behavior of bacteria, Limnol. Oceanogr. 46, 1309–1318, 2001.

Kiørboe, T., Grossart, H.-P., Ploug, H., and Kam T.: Bacterial colonization of sinking aggregates: mechanisms and rates, Appl. Environ. Microbiol., 68, 3996–4006, 2002.

Klaas, C. and Archer, D.: Association of sinking organic matter with various types of mineral ballast in the deep sea: Implications for the rain ratio. Global Biochem. Cycles, 16, 1–14, 2002.

Larsen, J. B., Larsen, A., Thyrhaug, R., Bratbak, G., and Sandaa, R.-A.: Response of marine viral populations to a nutrient induced phytoplankton bloom at different pCO_2 levels, Biogeosciences, 5, 523–533, 2008, http://www.biogeosciences.net/5/523/2008/.

Ledyard, K. M. and Dacey, J. W. H.: Dimethylsulfide production from dimethylsulfonioprpionate by a marine bacterium, Mar. Ecol. Prog. Ser., 110, 95–103, 1994.

Martens, T., Kessler, D., Gram, L., Grossart, H.-P., Simon, M., and Brinkhoff, T.: Bacteria of the Roseobacter clade show high potential for secondary metabolite production, Microb. Ecol., 54, 31–42, 2007.

Martinez, J., Smith, D. C., Steward, G. F., and Azam, F.: Variability in ectohydrolytic enzyme activities of pelagic marine bacteria and its significance for substrate processing in the sea, Aquat. Microb. Ecol., 10, 223–230, 1996.

McCune, B. and Grace, J.B.: Analysis of Ecological Communities, MjM Software Design, Glenden Beach, OR, 2002.

Muyzer, G., Dewaal, E. C., and Uitterlinden, A. G.: Profiling of complex microbial populations by denaturing gradient gel electrophoresis analysis of polymerase chain reaction-amplifies genes coding for 16S ribosomal-RNA, Appl. Environ. Microbiol., 59, 695–700, 1993.

Muyzer, G., Brinkhoff, T., Nübel, U., Santegoeds, C., Schäfer, H., and Wawer, C.: Denaturing gradient gel electrophoresis (DGGE) in microbial ecology, in: Molecular microbial ecology manual, edited by: Akkerman, A.D.L., van Elsas, J.D., and Bruijn, F.J., Kluwer Academic Publishers, Dordrecht, 1998.

Obernosterer, I. and Herndl, G. J.: Phytoplankton extracellular release and bacterial growth: Dependence on the inorganic N:P ratio, Mar. Ecol. Progr. Ser., 116, 247–257, 1995.

Passow, U.: Production of transparent exopolymer particles (TEP) by phyto- and bacterioplankton, Mar. Ecol.-Prog. Ser., 236, 1–12, 2002.

Paulino, A. I., Egge, J. K., and Larsen, A.: Effects of increased atmospheric CO_2 on small and intermediate sized osmotrophs during a nutrient induced phytoplankton bloom, Biogeosciences, 5, 739–748, 2008, http://www.biogeosciences.net/5/739/2008/.

Riebesell, U., Zondervan, I., Rost, B., Tortell, P. D., Zeebe, R. E., and Morel, F. M. M.: Reduced calcification in marine plankton in response to increased atmospheric CO_2, Nature, 407, 634–637, 2000.

Riebesell, U., Schulz, K. G. , Bellerby, R. G. J., Fritsche, P., Meyerhöfer, M., Neill, C., Nondal, G., Oschlies, A., Wohlers, J., and Zöllner, E.: Enhanced biological carbon consumption in a high CO_2 ocean, Nature, 450, 545–458, doi:10.1038/nature06267, 2007.

Riebesell, U., Bellerby, R. G. J., Grossart, H.-P., and Thinstad, F.: Mesocosm CO_2 perturbation studies: from organism to community level. Biogeosciences Discuss., 5, 641–659, 2008, http://www.biogeosciences-discuss.net/5/641/2008/.

Schulz, K. G., Riebesell, U., Bellerby, R. G. J., Biswas, H., Meyerhfer, M., Müller, M. N., Egge, J. K., Nejstgaard, J. C., Neill, C., Wohlers, J., and Zöllner, E.: Build-up and decline of organic matter during PeECE III, Biogeosciences, 5, 707–718, 2008, http://www.biogeosciences.net/5/707/2008/.

Simó, R., Archer, S. D., Pedros-Alio, C., Gilpin, L., and Stelfox-Widdicombe, C. E.: Coupled dynamics of dimethylsulfoniopropionate and dimethylsulfide cycling and the microbial food web in surface waters of the North Atlantic, Limnol. Oceanogr., 47, 53–61, 2002.

Simon, M., Grossart, H.-P., Schweitzer, B., and Ploug, H.: Microbial Ecology of Organic Aggregates in Aquatic Ecosystems, Aquat. Microb. Ecol, 28, 175–211, 2002.

Smith, D. C., Simon, M., Alldredge, A. L., and Azam, F.: Intense hydrolytic enzyme-activity on marine aggregates and implications for rapid particle dissolution, Nature, 359, 139–142, 1992.

Smith, D. C., Steward, G. F., Long, R. A., and Azam, F.: Bacterial mediation of carbon fluxes during a diatom bloom in a mesocosm, Deep-Sea Res., 42, 75–97, 1995.

Søndergaard, M., Williams P. J. le B., Cauwet, G., Riemann, B., Robinson, C., Terzic, S., Woodward E. M. S., and Worm, J.: Net accumulation and flux of dissolved organic carbon and dissolved organic nitrogen in marine plankton communities, Limnol. Oceanogr., 45, 1097–1111, 2000.

Stefels, J., Dijkhuizen, L., and Gieskes, W. W. C.: DMSP-lyase activity in a spring phytoplankton bloom off the Dutch coast, related to *Phaeocystis sp.* abundance, Mar. Ecol. Prog. Ser., 123, 235–243, 1995.

Stefels, J.: Physiological aspects of the production and conversion of DMSP in marine algae and higher plants, J. Sea Res., 43, 183–197, 2000.

Stefels, J., Steinke, M., Turner, S., Malin, G., Belviso, S.: Environmental constraints on the production and removal of the climatically active gas dimethylsulfide (DMS) and implications for ecosystem modelling, Biogeochemistry, 83, 245–275, 2007.

Steinke, M., Wolfe, G. V., and Kirst, G. O.: Partial characterisation of dimethylsulfoniopropionate (DMSP) lyase isozymes in 6 strains of *Emiliania huxleyi*, Mar. Ecol. Prog. Ser., 175, 215–225, 1998.

Steinke, M., Malin, G., Archer, S. D., Burkill, P. H., and Liss, P. S.: DMS production in a coccolithophorid bloom: evidence for the importance of dinoflagellate DMSP lyases, Aquat. Microb. Ecol., 26, 259–270, 2002.

Sunda, W., Kieber, D. J., Kiene, R. P., and Huntsman, S.: An antioxidant function for DMSP and DMS in marine algae. Nature, 418, 317–320, 2002.

Tanaka, T., Thingstad, T. F., Løvdal, T., Grossart, H.-P., Larsen, A., Allgaier, M., Meyerhöfer, M., Schulz, K. G., Wohlers, J., Zöllner, E., and Riebesell, U.: Availability of phosphate for phytoplankton and bacteria and of glucose for bacteria at different pCO_2 levels in a mesocosm study, Biogeosciences, 5, 669–678, 2008,

http://www.biogeosciences.net/5/669/2008/.

Thingstad, F. T., Hagström, A., and Rassoulzadegan, F.: Accumulation of degradable DOC in surface waters: Is it caused by a malfunctioning microbial loop?, Limnol. Oceanogr., 42, 398–404, 1997.

Thinstad, T. F.: Elements of a theory for the mechanisms controlling abundance, diversity, and biogeochemical role of lytic bacterial viruses in aquatic systems, Limnol. Oceanogr., 45, 1320–1328, 2000.

Todd, J. D., Rogers, R., Li, Y. G., Wexler, M., Bond, P. L., Sun, L., Curson, A. R. J., Malin, G., Steinke, M., and Johnston, A. W. B.: Structural and regulatory genes required to make the gas dimethyl sulfide in bacteria. Science, 315, 666–669, 2007.

Tortell, P. D., Ditullio, G. R., Sigmann, D. M., and Morel, F. M. M.: CO_2 effects on taxonomic composition and nutrient utilization in an Equatorial Pacific phytoplankton assemblage, Mar. Ecol. Prog. Ser., 236, 37-43, 2002.

Vila-Costa, M., del Valle, D., González, J. M., Slezak, D., Kiene, R. P., Sánchez, O., Simó, R.: Phylogenetic identification and metabolism of marine dimethylsulfide-consuming bacteria, Environ. Microbiol., 8, 2189–2200, 2007a.

Vila-Costa, M., del Pinhassi, J., Alonso, C., Pernthaler, J., Simó, R.: An annual cycle of dimethylsulfoniopropionate-sulfur and leucine assimilating bacterioplankton in the coastal NW Mediterranean, Environ. Microbiol., 9, 2451–2463, 2007b.

Vogt, M., Steinke, M., Turner, S., Paulino, A., Meyerhöfer, M., Riebesell, U., LeQuërë, C., and Liss, P.: Dynamics of dimethylsulphoniopropionate and dimethylsulphide under different CO_2 concentrations during a mesocosm experiment, Biogeosciences, 5, 407–419, 2008, http://www.biogeosciences.net/5/407/2008/.

Williams, P. J. le B.: Evidence for the seasonal accumulation of carbon-rich dissolved organic material, its scale in comparison with changes in particulate material and the consequential effect on net C/N assimilation ratios, Mar. Chem., 51, 17–29, 1995.

Wilson, W. H., Tarran, G. A., Schroeder, D., Cox, M., Oke, J., and Malin, G.: Isolation of a virus responsible for the demise of an *Emiliania huxleyi* bloom in the English Channel, J. Mar. Biol. Assoc. UK, 82, 369–377, 2002.

Wolf-Gladrow, D., Riebesell, U., Burkhardt, S., and Bijma, J.: Direct effect of CO_2 concentration on growth and isotopic composition of marine plankton, Tellus, 51B, 461–476, 1999.

Zak, D. R., Pregitzer, K. S., Curtis, P. S., and Holmes, W. E.: Atmospheric CO_2 and the composition of soil microbial communities, Ecol. Appl., 10: 47–59.

Zhou, J., Mopper, K., and Passow, U.: The role of surface-active carbohydrates in the formation of transparent exopolymer particles by bubble adsorption of seawater, Limnol. Oceanogr., 43, 1860–1871, 1998.

Zubkov, M. V., Fuchs, B. M., Archer, S. D., Kiene, R. P., Amann, R., and Burkill, P. H.: Linking the composition of bacterioplankton to rapid turnover of dissolved dimethylsulfoniopropionate in an algal bloom in the North Sea, Environ. Microbiol., 3, 304–311, 2001.